



Sandia
National
Laboratories

Exceptional service in the national interest

ME469: Multiphase Methods: Volume of Fluid Methods

Stefan P. Domino^{1,2}

¹ Computational Thermal and Fluid Mechanics, Sandia National Laboratories

² Institute for Computational and Mathematical Engineering, Stanford

This presentation has been authored by an employee of National Technology & Engineering Solutions of Sandia, LLC under Contract No. DE-NA0003525 with the U.S. Department of Energy (DOE). The employee owns all right, title and interest in and to the presentation and is solely responsible for its contents. The United States Government retains and the publisher, by accepting the article for publication, acknowledges that the United States Government retains a non-exclusive, paid-up, irrevocable, world-wide license to publish or reproduce the published form of this article or allow others to do so, for United States Government purposes. The DOE will provide public access to these results of federally sponsored research in accordance with the DOE Public Access Plan <http://www.energy.gov/downloads/doe-public-access-plan>.

SAND2018-4536 PE





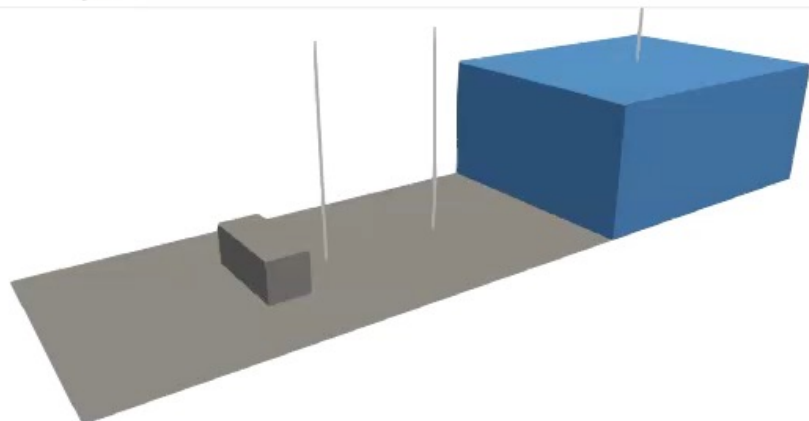
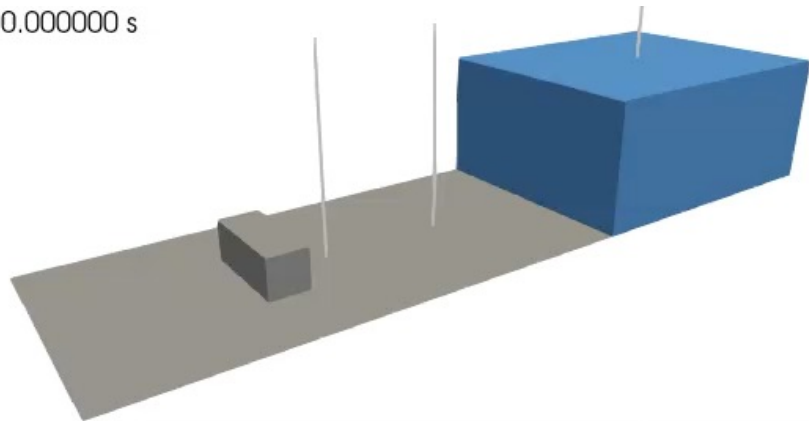
Objective: Model Multiphase Flow (Air/Water)

Validation case of Kleefsman et al.
"A volume-of-fluid based simulation
method for wave impact problems",
J. Comput. Phys. (2005).

See:

[/laboratory/3d_hex8_dam_break](#)

Time: 0.000000 s



Step 1: Definition of an Water/Air interface (Phase 1/Phase 2)

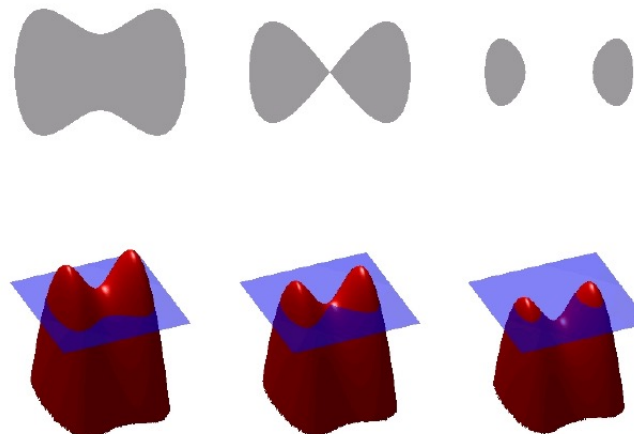
Signed-distance function (level-set), Ψ

- Popularized by Osher and Sethian, "Fronts propagating with curvature-dependent speed: Algorithms based on Hamilton-Jacobi formulations", J. Comp. Phys., 1988,

Volume of Fluid, ϕ or α

- Lineage classically provided to Noh, W.F.; Woodward, P. (1976). van de Vooren, A.I.; Zandbergen, P.J. (eds.). *SLIC (Simple Line Interface Calculation). proceedings of 5th International Conference of Fluid Dynamics. Lecture Notes in Physics. Vol. 59. pp. 330-340*
- Interpretation: volume fraction of phase 1, interphase lives at $\frac{1}{2}$

$$\rho = \alpha \rho^{\alpha=1} + (1 - \alpha) \rho^{\alpha=0} \quad \frac{\partial \alpha}{\partial t} + u_j \frac{\partial \alpha}{\partial x_j} = 0$$



Ψ defines an zero-isocontour, with distance (+/- in either direction)

$$n_j^I = \frac{\frac{\partial \alpha}{\partial x_j}}{\left| \frac{\partial \alpha}{\partial x_j} \right|} \quad \kappa = -\frac{\partial n_j^I}{\partial x_j}$$

Interface normal and curvature



Definition of an Water/Air interface (Phase 1/Phase 2)

Signed-distance function (level-set), Ψ

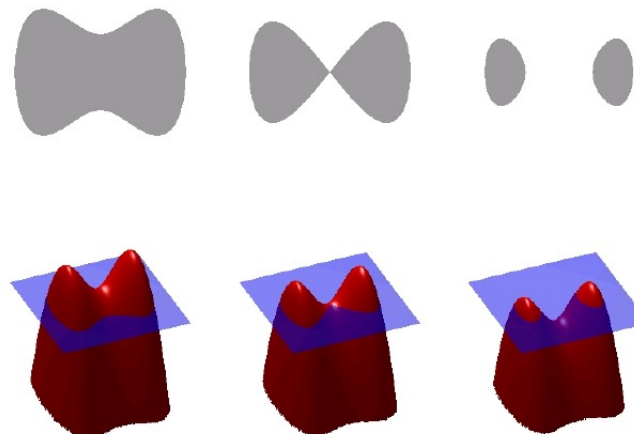
- Popularized by Osher and Sethian, "Fronts propagating with curvature-dependent speed: Algorithms based on Hamilton-Jacobi formulations", J. Comp. Phys., 1988,

Volume of Fluid, ϕ or α

- Lineage classically provided to Noh, W.F.; Woodward, P. (1976). van de Vooren, A.I.; Zandbergen, P.J. (eds.). *SLIC (Simple Line Interface Calculation)*. proceedings of 5th International Conference of Fluid Dynamics. Lecture Notes in Physics. Vol. 59. pp. 330-340
- Interpretation: volume fraction of phase 1, interphase lives at $\frac{1}{2}$

$$\rho = \alpha \rho^{\alpha=1} + (1 - \alpha) \rho^{\alpha=0}$$

$$\frac{\partial \alpha}{\partial t} + u_j \frac{\partial \alpha}{\partial x_j} = 0$$



Ψ defines an zero-isocontour, with distance (+/- in either direction)

$$n_j^I = \frac{\frac{\partial \alpha}{\partial x_j}}{\left| \frac{\partial \alpha}{\partial x_j} \right|} \quad \kappa = - \frac{\partial n_j^I}{\partial x_j}$$

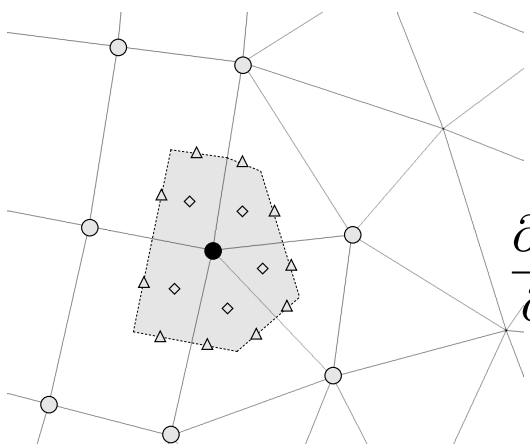
Interface normal and curvature

VOF Transport Discretization Nuance: Volume- or Surface-based?

- Simple enough, define the volume (fraction) of fluid (absent evaporation): $\frac{\partial \alpha}{\partial t} + u_j \frac{\partial \alpha}{\partial x_j} = 0$

Option 1: volumetric-form: $\int \frac{\partial \alpha}{\partial t} dV + \int u_j \frac{\partial \alpha}{\partial x_j} dV = 0$

CVFEM/FEM (really, any element-based approach)
Evaluated as a volumetric-contribution (diamonds)



$$\phi_{ip} = \sum_n N_n^{ip} \phi_n$$

$$\frac{\partial \phi_{ip}}{\partial x_j} = \sum_n \frac{\partial N_n^{ip}}{\partial x_j} \phi_n$$

Option 2: divergence-form:

$$\int \frac{\partial \alpha}{\partial t} dV + \int \frac{\partial \alpha u_j}{\partial x_j} dV - \int \alpha \frac{\partial u_j}{\partial x_j} dV = 0$$

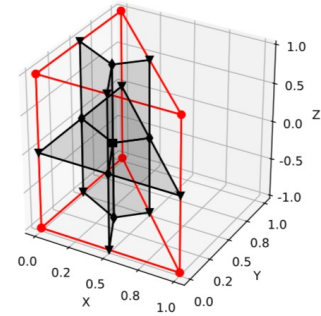
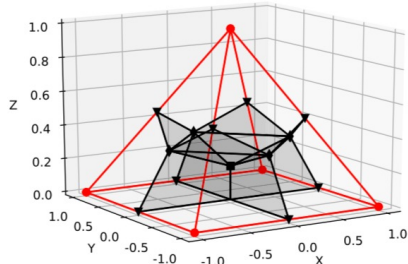
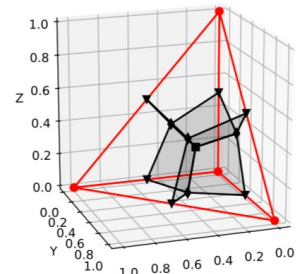
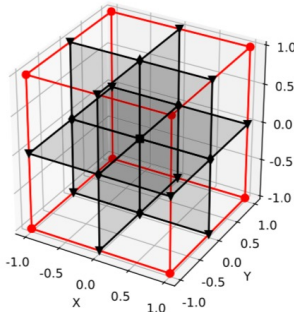
↓
Gauss-Divergence $\int \alpha \hat{u}_j n_j dS$

Traditional finite volume (element, edge, cell-centered)
Evaluated as a surface integral (triangle)

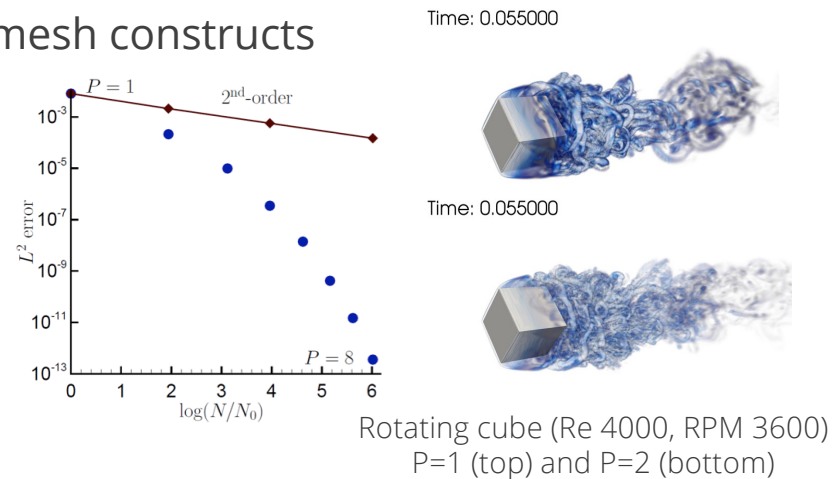
Allows for a consistent advecting velocity (mass conserving)
that is obtained from the continuity equation

Baseline: Generalized, Unstructured Numerical Formulation

- Objective: Scalable, Efficient fluids on hybrid-based mesh constructs



Control-volume finite-element method (CVFEM)



- CVFEM can be viewed as Petrov-Galerkin method (basis differs from test function)
- High-quality on generalized unstructured meshes, Domino et al. Comput. Fluids (2019)
- The method can also be promoted in polynomial space, see Domino, CTRSP (2014) as a first example of low-Mach fluids algorithm – or Domino, J. Comp. Phys. (2018)
 - GPU, Knaus, Comput. Fluids (2022)



Equal-Order Interpolation, i.e., Collocation: Pressure Stabilization Review (1/2)

- A variety of forms/explanations – depending on the particular community; at its base:

$$\int \left(\frac{\partial \rho^{k+1} u_i^{k+1}}{\partial t} + G_i p^k \right) dV + \int \rho^{k+1} \hat{u}_j u_i^{k+1} n_j dS \\ = \int 2\mu S_{ij}^{*k+1} n_j dS + \int F_i dV$$

$$\int w G_j \phi dV = \int w \frac{\partial \phi}{\partial x_j} dV$$

Projected nodal gradient that
can be mass-lumped

$$\int \frac{\partial \rho^{k+1}}{\partial t} dV + \int \rho^{k+1} \hat{u}_j n_j dS = 0$$

What is \hat{u}_j ? (next slide)?



Equal-Order Interpolation, i.e., Collocation: Pressure Stabilization Review (2/2)

- \hat{u}_j is a function of the fine-scale momentum residual (evaluated at an integration point):

$$\hat{u}_j = u_j - \frac{\tau}{\rho} R^h(u_j) \quad R^h(u_j) = \frac{\partial \rho u_i}{\partial t} + \frac{\partial \rho u_j u_i}{\partial x_j} - \frac{\partial}{\partial x_j} 2\mu S_{ij}^* + \frac{\partial p}{\partial x_i} - F_i \quad (1)$$

We can also project this residual to the nodes, $\hat{R}^h(u_j) = T_i + A_i - D_i + G_i - F_i$ and approximate $R^h(u_j)$ as re-interpolation of choice terms

- Usage of a full residual (1) results in a classic Pressure Stabilized Petrov Galerkin (Hughes et al. 1986)
- Pick and choose each residual, Majumdar (1988)
- Algebraically manipulation affords the classic Rhie-Chow-based (1983) pressure stabilization

$$\hat{u}_j = u_j - \frac{\tau}{\rho} \left(\frac{\partial p}{\partial x_j} - G_j p \right)$$

- shown to be stable and dissipative [Ham and Iaccarino (2004) or Domino (2006)]

- There is also the nuance of pressure projection vs monolithic



VOF Transport: Sharpening + Advection Stabilization + Interface Smoothing

VOF equation with PDE-based sharpening (to mitigate numerical diffusion) that includes residual-based stabilization

$$\int \frac{\partial \alpha}{\partial t} dV + \int \alpha \hat{u}_j n_j dS - \int \frac{\partial s_j}{\partial x_j} dV - \sum_e \int \tau^h u_j^R R^h(\alpha) n_j dS - \sum_e \int \nu^h g^{ij} \frac{\partial \alpha}{\partial x_j} n_i dS = 0$$

$$n_j^I = \frac{\sum_{scv} \left(\frac{\partial \alpha}{\partial x_j} \right)_{scv} V_{scv}}{\left(\left\| \frac{\partial \alpha}{\partial x_j} \right\|_{scv} + \epsilon \right) \sum_{scv} V_{scv}}$$

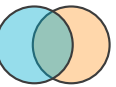
Integrated-by-parts advection to allow for consistent continuity constraint; $R^h(\alpha)$

PDE-based sharpening with compression velocity $s_j = -u_{c_j} \alpha (1 - \alpha)$
in the direction of the interface normal, n_j^I $u_{c_j} = C_\alpha |u_k - v_k| n_j^I$

Streamwise-upwind, control volume (SUCV), Swaminathan et al., Int. J. Numer. Meth. Engr. (1993); based on Streamwise Upwind Petrov-Galerkin (SUPG), Brooks and Hughes, Comput. Methods in Appl. Mech. Eng. (1982).

Nonlinear stabilization operator (NSO); Motivated by Shakib et. al, Comput. Methods in Appl. Mech. Eng. (1991), discontinuity capturing operator (later termed NSO); $\nu^h = f(R^h(\alpha))$ NSO and SUCV avoids common gradient reconstruction techniques commonly used in unstructured formulations, see Tsui et al., Int. J. Heat Mass Trans. (2009)

Nuance: interface normal can be computed using a smoothed VOF field



VOF using Balanced Force: Brief Survey

- First CVFEM: Lin et al, J. Comput. Phys. (2019)
- Classic Balanced Force, Francois, J. Comput. Phys. (2006) ported to CVFEM
- Parasitic currents suppressed via a consistent momentum/continuity stabilization form: fine-scale momentum residual algebraically modified in continuity equation
 - Note: not trying to pioneer a novel balanced force approach

$$\begin{aligned}
 & \int \left(\frac{\partial}{\partial t} \rho^* u_i^{k+1} + \rho^* \hat{G}_i p^k \right) dV + \int \rho^* \hat{u}_j u_i^{k+1} n_j dS \\
 &= \int \mu^* \left(\frac{\partial u_i^{k+1}}{\partial x_j} + \frac{\partial u_j^{k+1}}{\partial x_i} \right) n_j dS + \int \gamma \rho^* g_i dV
 \end{aligned}
 \quad \left| \begin{array}{l} \hat{G}_\beta p^k = \frac{\sum_{ip} \frac{1}{\rho^*} \left(\frac{\partial p^k}{\partial x_\beta} - \sigma \kappa \frac{\partial \alpha}{\partial x_\beta} - \gamma \rho^* g_\beta \right) |A_\beta|}{\sum_{ip} |A_\beta|} \\ \text{Nodal pressure gradient} \end{array} \right.$$

Momentum Equation

$$- \int \frac{1}{\rho^*} \frac{\partial \Delta p^{k+1}}{\partial x_j} n_j dS = - \frac{1}{\Delta t} \int \hat{u}_j n_j dS$$

Continuity Equation

$$\hat{u}_j = u_j^{R,k} - \Delta t \left(\frac{1}{\rho^*} \left(\frac{\partial p^k}{\partial x_j} - \sigma \kappa \frac{\partial \alpha}{\partial x_j} - \gamma \rho^* g_j \right) - \hat{G}_j p^k \right)$$

Convection-velocity

Note: benefits from ρg_i ($\gamma = 1$) included in stabilization

VOF using Balanced Force: Leveraging Existing Approaches

- First CVFEM: Lin et al, J. Comput. Phys. (2019)
- Classic Balanced Force, Francois, J. Comput. Phys. (2006) ported to CVFEM
- Parasitic currents suppressed via a consistent momentum/continuity stabilization form: fine-scale momentum residual algebraically modified in continuity equation
 - Note: not trying to pioneer a novel balanced force approach

$$\int \left(\frac{\partial}{\partial t} \rho^* u_i^{k+1} + \rho^* \hat{G}_i p^k \right) dV + \int \rho^* \hat{u}_j u_i^{k+1} n_j dS$$

$$\hat{G}_\beta p^k = \frac{\sum_{ip} \frac{1}{\rho^*} \left(\frac{\partial p^k}{\partial x_\beta} - \sigma \kappa \frac{\partial \alpha}{\partial x_\beta} - \gamma \rho^* g_\beta \right) |A_\beta|}{\sum_{ip} |A_\beta|}$$

Surface tension Continuum Surface Force (CSF)

$$= \int \mu^* \left(\frac{\partial u_i^{k+1}}{\partial x_j} + \frac{\partial u_j^{k+1}}{\partial x_i} \right) n_j dS + \int \gamma \rho^* g_i dV$$

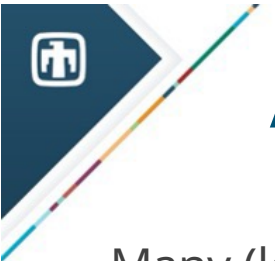
Momentum Equation

$$- \int \frac{1}{\rho^*} \frac{\partial \Delta p^{k+1}}{\partial x_j} n_j dS = - \frac{1}{\Delta t} \int \hat{u}_j n_j dS$$

Continuity Equation

$$\hat{u}_j = u_j^{R,k} - \Delta t \left(\frac{1}{\rho^*} \left(\frac{\partial p^k}{\partial x_j} - \sigma \kappa \frac{\partial \alpha}{\partial x_j} - \gamma \rho^* g_j \right) - \hat{G}_j p^k \right)$$

Note: benefits from ρg_i ($\gamma = 1$) included in stabilization



A Note on Methods and CSF

Many (local!!) experts:

- Jain et al., A conservative diffuse-interface method for compressible two-phase flows, J. Comp. Phys, 2020.
- Jain, "Accurate conservative phase-field method for simulation of two-phase flows, J. Comp. Phys, 2022.
- Mirjalili et al., Assessment of an energy-based surface tension model for simulation of two-phase flows using second-order phase field methods, J. Comp. Phys. 2023.
- Huang and Jain, "A phase-filed method for simulations of two-phase flows on unstructured grids", Annual CTR Briefs, 2022.
- Barbeau and Lele, Assessment of Localized Artificial Diffusivity (LAD) and Interface Sharpening for Modelling a Two-Phase Mixing Layer, PSAAP-3 Poster Session.

3. Modeling & Computational Approach

- Diffuse interface method using 4 equation model with surface tension, Localized Artificial Diffusivity (LAD), and interface sharpening terms
- **Time Advancement:** 4th order, 5 stage RK method in time
- **Spatial Discretization:** 10th order penta-diagonal, compact finite difference scheme used unless otherwise stated
- **Interface Sharpening Discretization:** 2nd order central difference using a staggered approach¹. Conservative Diffuse Interface¹ (CDI) and Accurate Conservative Diffuse Interface² (ACDI) methods are considered
- **LAD:** used for interface regularization when the artificial diffusivity D_m^* of a species is activated³

$$a_m = \nabla \cdot \left(\Gamma \left(\epsilon \nabla \phi - \phi (1 - \phi) \frac{\nabla \phi}{|\nabla \phi|} \right) \right) \xrightarrow{\text{ACDI}} a_m = \nabla \cdot \left(\Gamma \left(\epsilon \nabla \phi - \frac{1}{4} \left(1 - \tanh^2 \left(\frac{\psi}{2\epsilon} \right) \right) \frac{\nabla \psi}{|\nabla \psi|} \right) \right)$$
$$\psi = \epsilon \ln \left(\frac{\phi + \epsilon}{1 - \phi + \epsilon} \right)$$

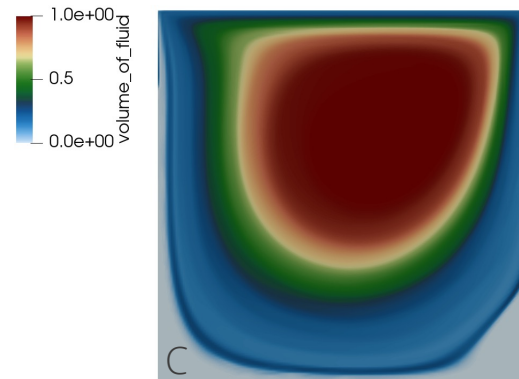
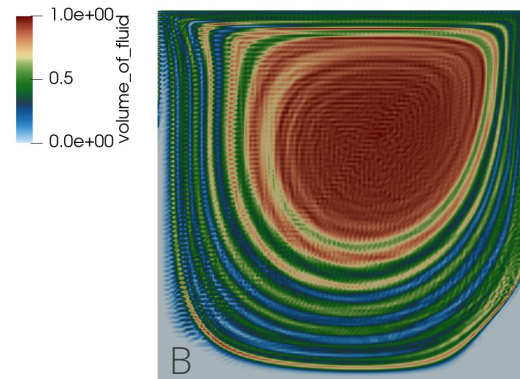
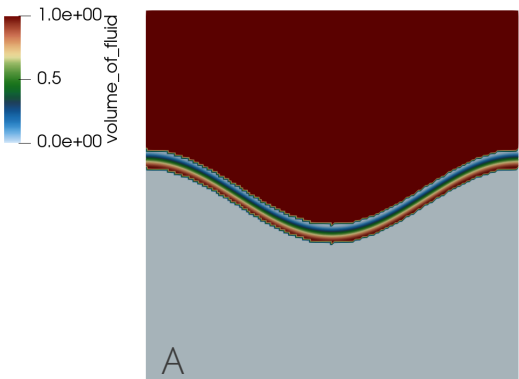
- **Surface Tension Modeling:** Continuum Surface Tension Force $F = \sigma \kappa \nabla \phi$

$$\begin{array}{lll} \text{CSF} & \psi \text{ CSF}^1 & \psi \text{ Localized CSF}^{1,4} \\ F = \sigma \nabla \cdot \frac{\nabla \phi}{|\nabla \phi|} \nabla \phi & F = \sigma \nabla \cdot \frac{\nabla \psi}{|\nabla \psi|} \nabla \phi & F = 6\sigma\phi(1-\phi)\nabla \cdot \frac{\nabla \psi}{|\nabla \psi|} \nabla \phi \end{array}$$

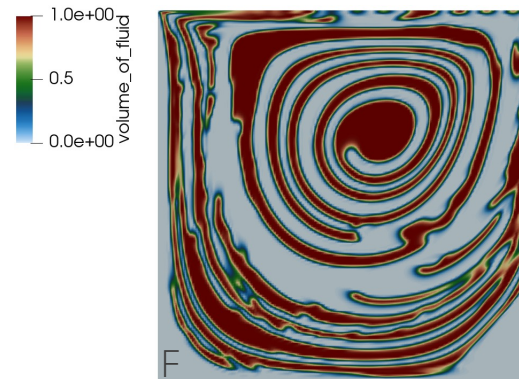
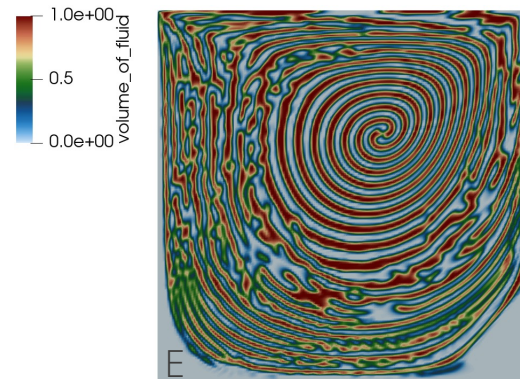
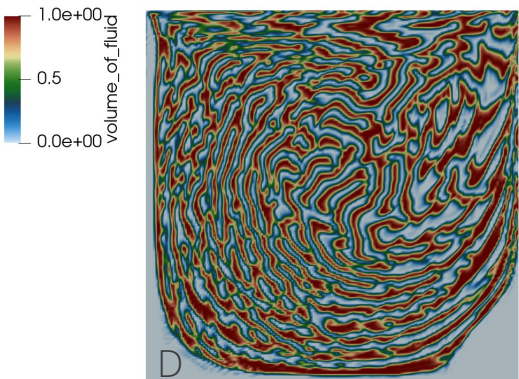


Passive Transport Example: Driven Cavity

- Exploring PDE-based sharpening, interface smoothing and stabilization

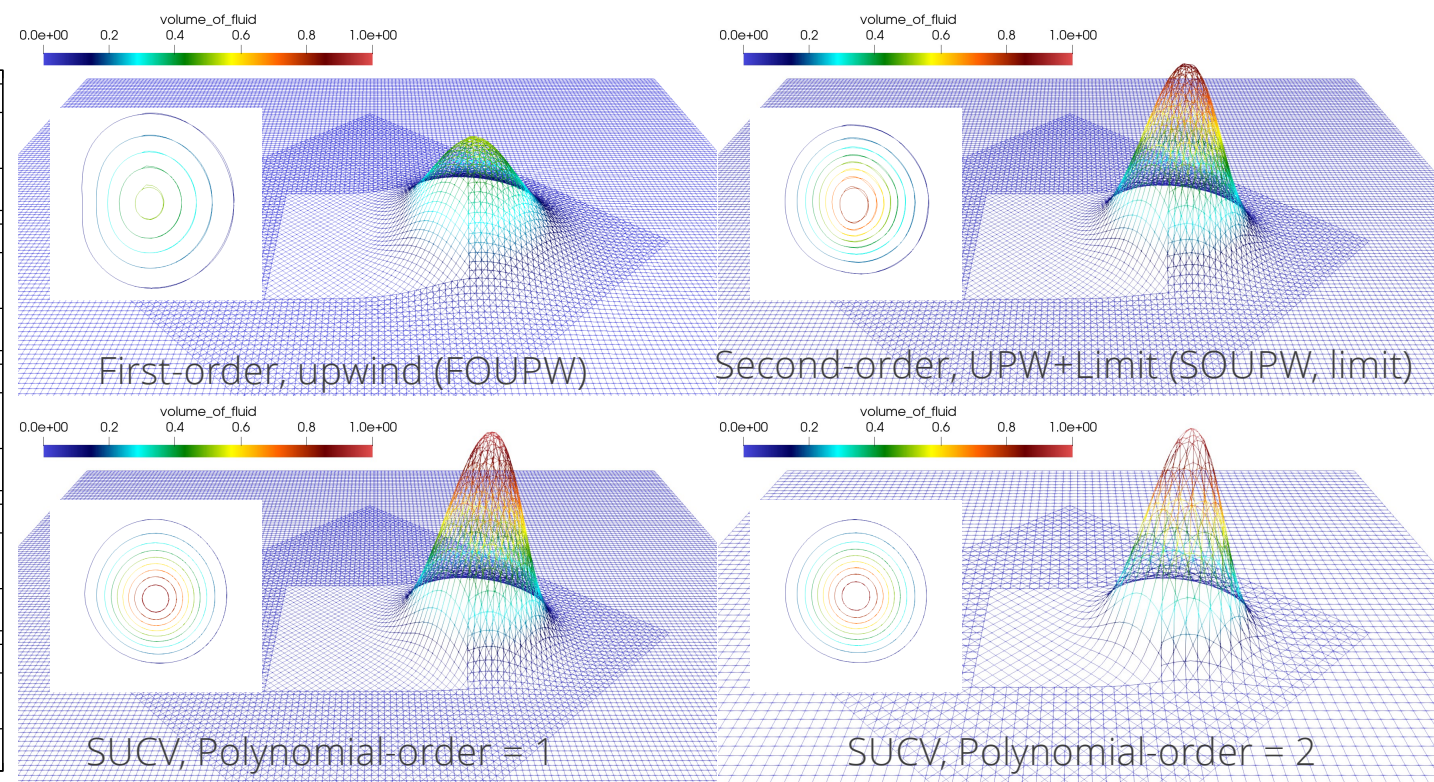
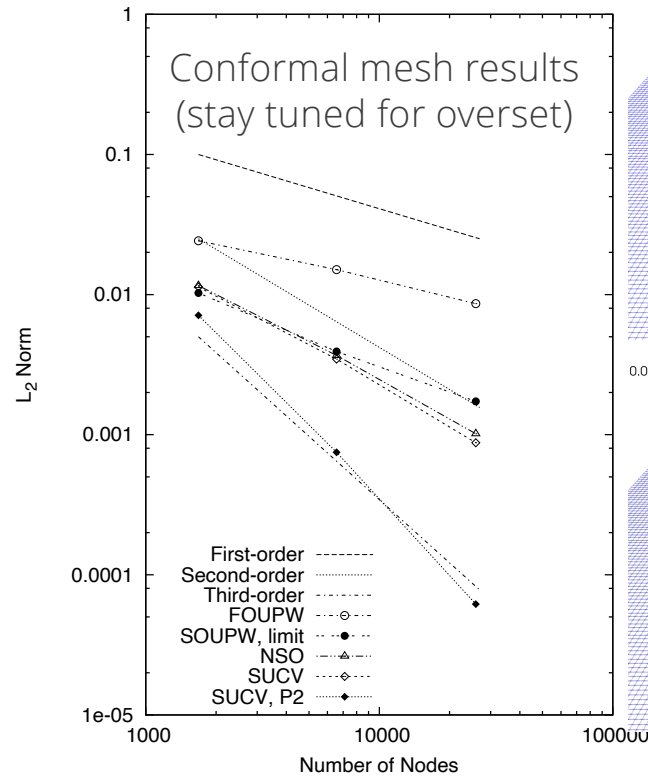


- A. Initial condition
- B. No stabilization
- C. SUCV+NSO
- D. Sharpening+B
- E. Sharpen+C
- F. E+Smoothing



Residual-based stabilization

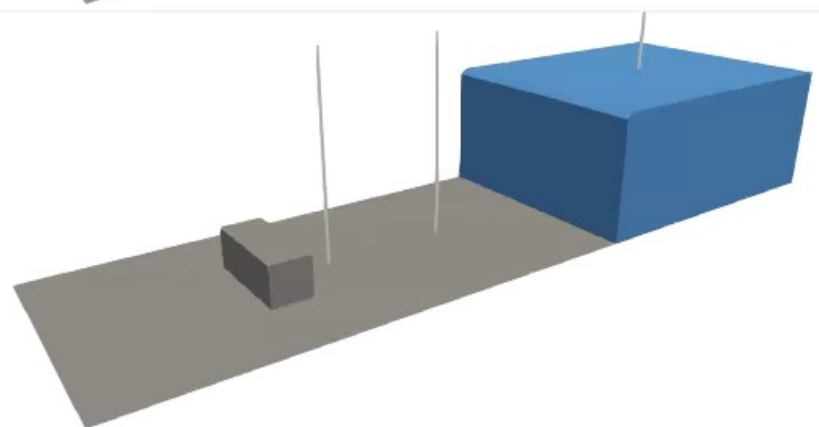
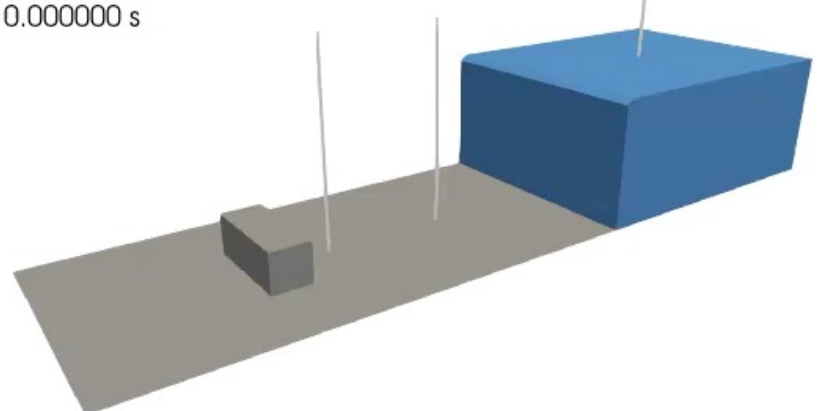
- Molenkamp verification, see Martinez, Int. J. Numer. Meth. Engr. (2004), with a variety of stabilization options





Dam Break Validation: The Benefit of a Full Balanced-Force Method

- Here, comparisons made between $\gamma = 1$ (top) and $\gamma = 0$ (bottom) showcasing the increased stabilizing effect of the set of all body forces in momentum included in the pressure stabilization formulation
- A nuance briefly captured and/or hinted at in seminal Francois et al., J. Comput. Phys. (2006) effort

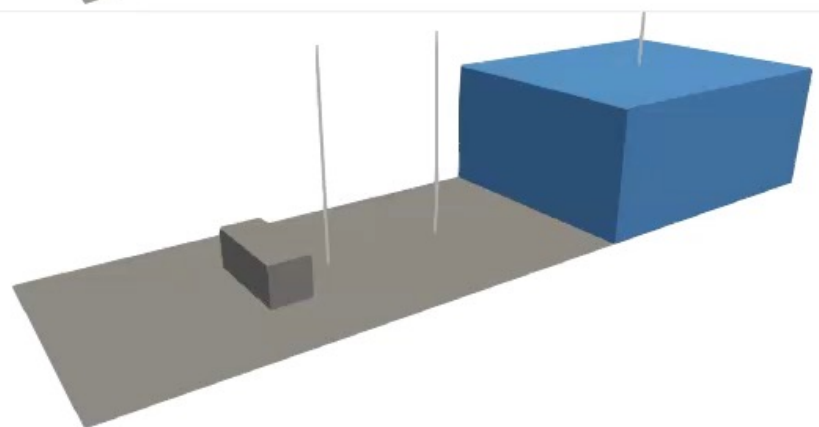
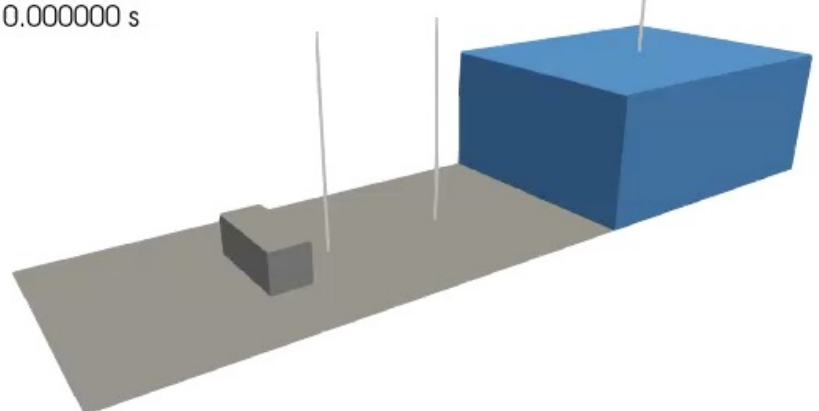


$$\hat{u}_j = u_j^{R,k} - \Delta t \left(\frac{1}{\rho^*} \left(\frac{\partial p^k}{\partial x_j} - \sigma \kappa \frac{\partial \alpha}{\partial x_j} - \gamma \rho^* g_j \right) - \hat{G}_j p^k \right)$$

R0

Dam Break Validation: The Benefit of a Full Balanced-Force Method

- Here, comparisons made between $\gamma = 1$ (top) and $\gamma = 0$ (bottom) showcasing the increased stabilizing effect of the set of all body forces in momentum included in the pressure stabilization formulation
- A nuance briefly captured and/or hinted at in seminal Francois et al., J. Comput. Phys. (2006) effort

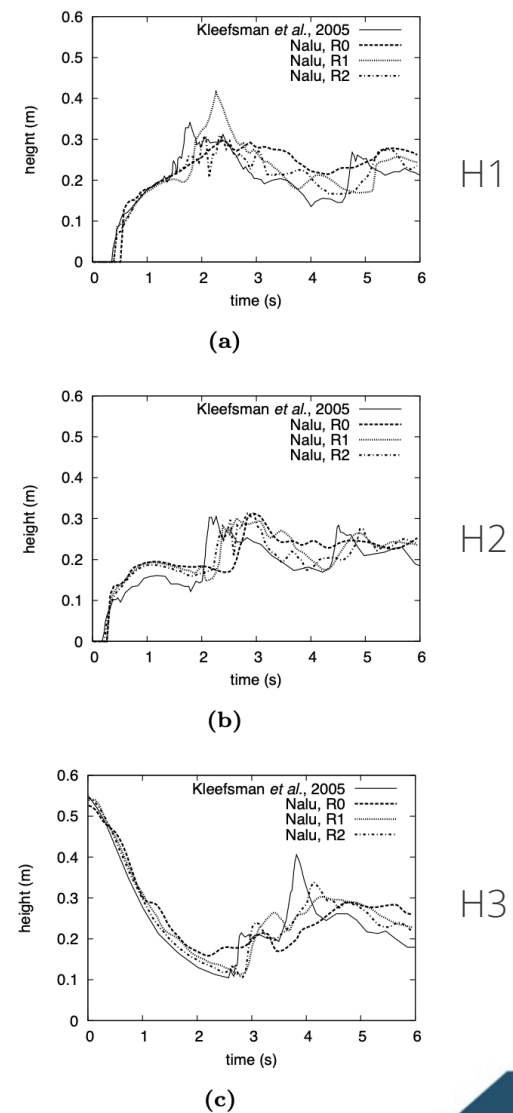
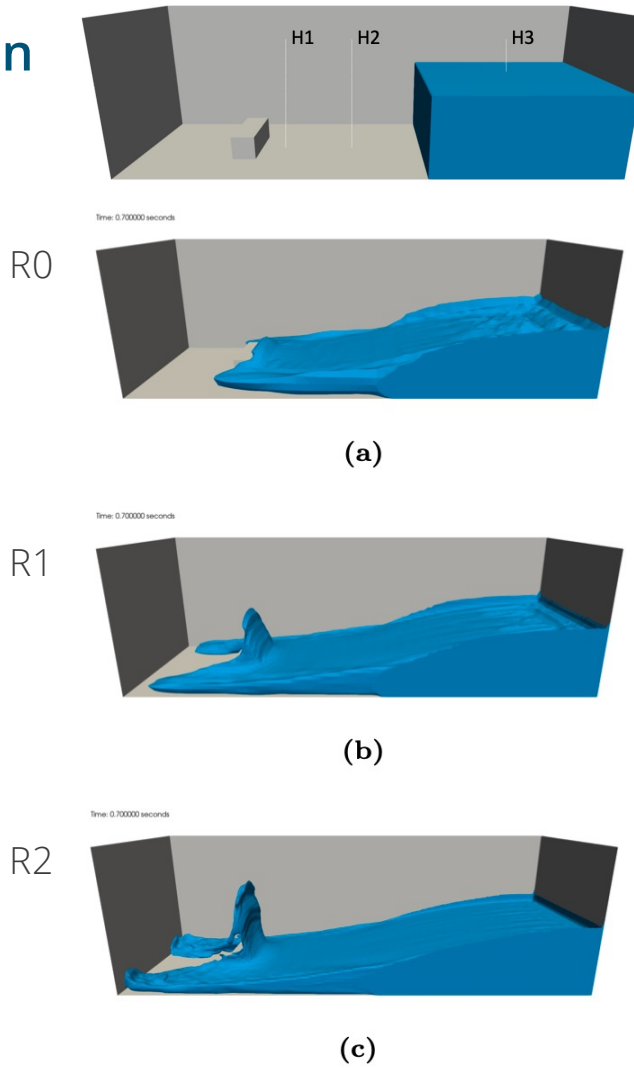


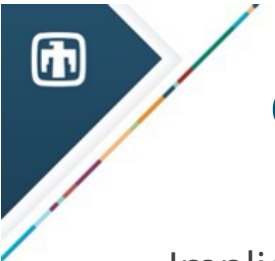
$$\hat{u}_j = u_j^{R,k} - \Delta t \left(\frac{1}{\rho^*} \left(\frac{\partial p^k}{\partial x_j} - \sigma \kappa \frac{\partial \alpha}{\partial x_j} - \gamma \rho^* g_j \right) - \hat{G}_j p^k \right) \quad R2$$



Dam Break Validation

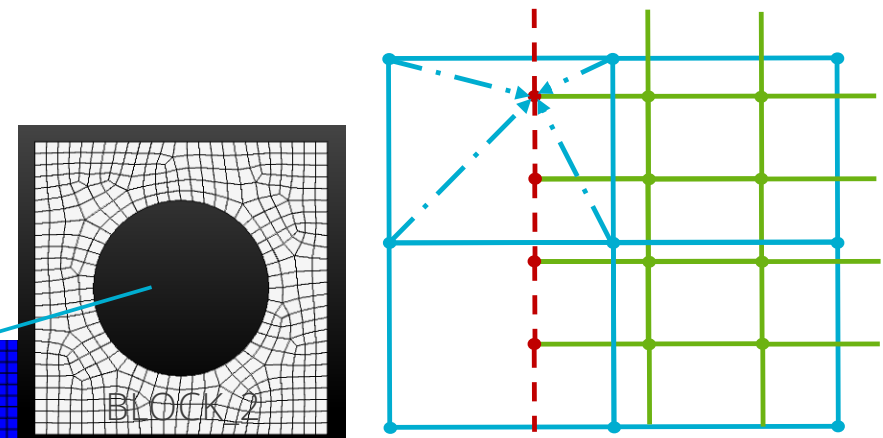
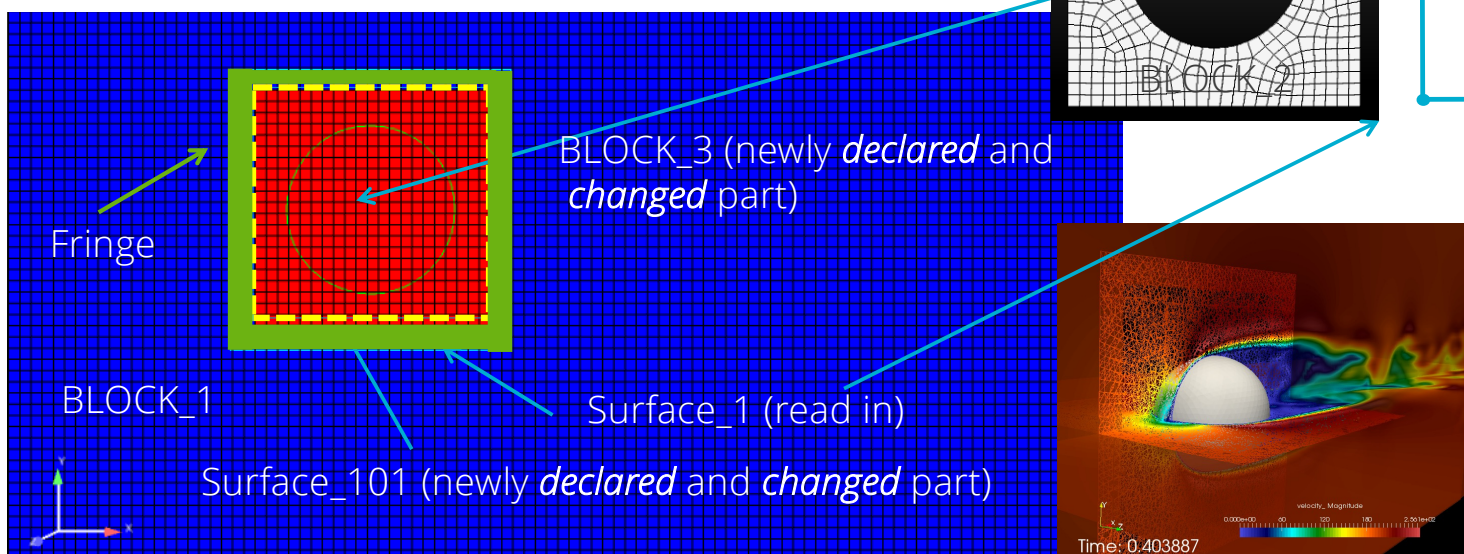
- Validation case of Kleefsman et al. "A volume-of-fluid based simulation method for wave impact problems", J. Comput. Phys. (2005).
- Qualitative comparisons also made to SNL's Sierra/Fuego, Brown et al. "Modeling a rubble fire consisting of comingled liquid and solid fuel", Tech. Rep. SAND2017-12318C (2017).



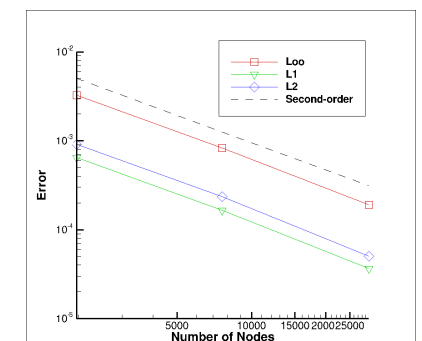


Overset: Freedom for Generalized Motion

- Implicit, constraint-based overset-based approach (DG/CVFEM-based, started)
- Does not require presumed movement**
- Similar to Nalu-Wind's Sharma et al, J. Comput. Phys. (2021), however, STK-based search



Constraint-based

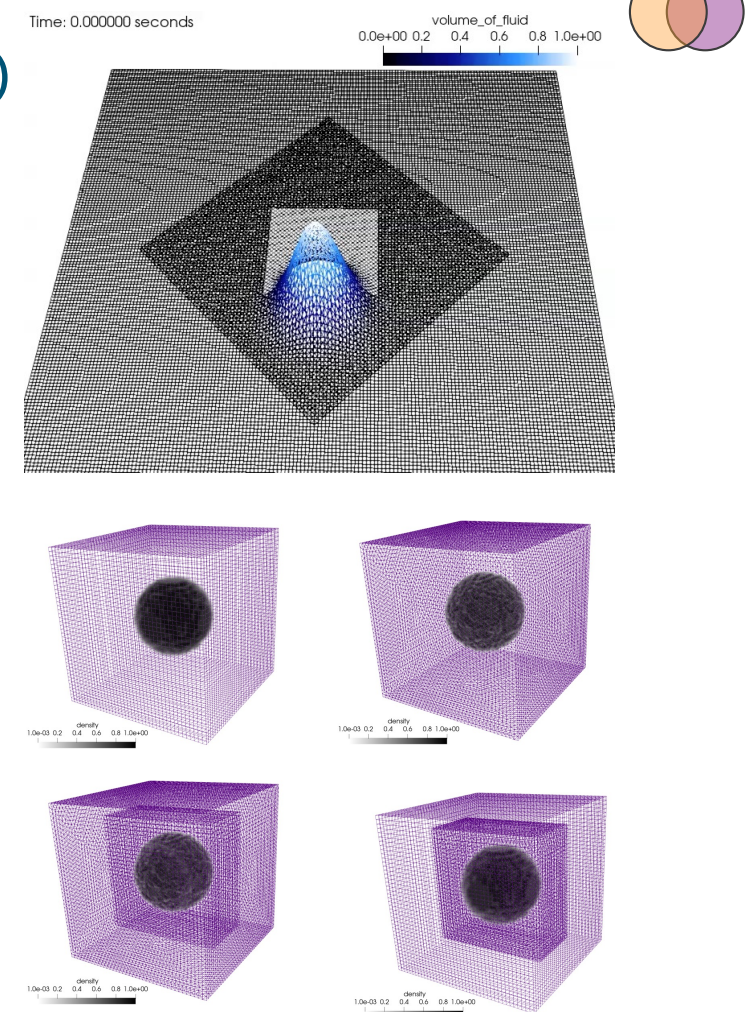
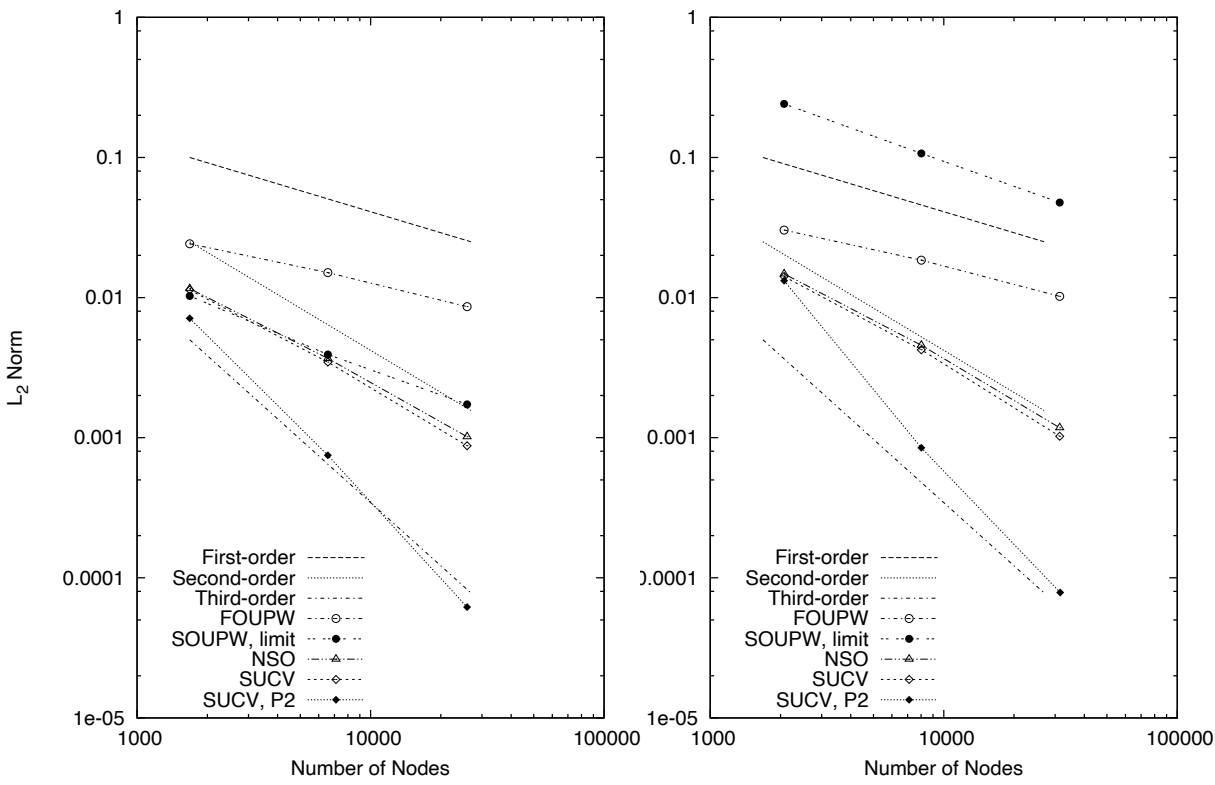


Fluids Hex/Tet

MMS

Objective: Overset + Volume of Fluid (VOF)

- Molenkamp verification case, now with overset
- Static bubble (computed curvature)

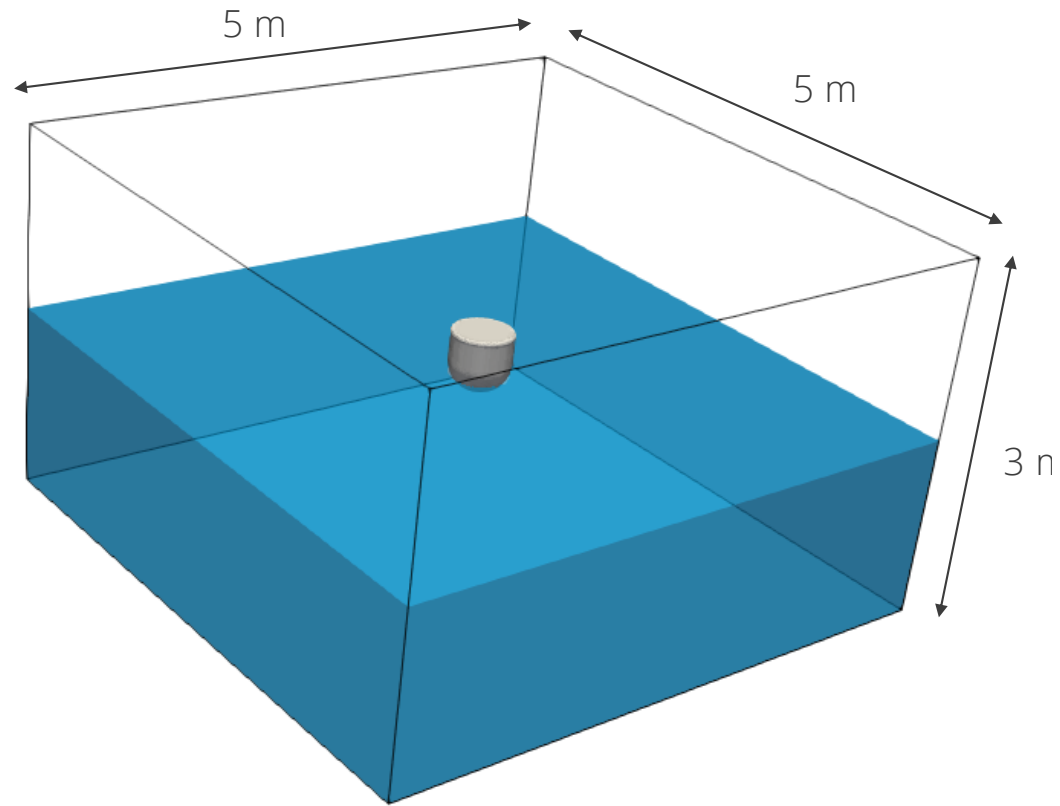
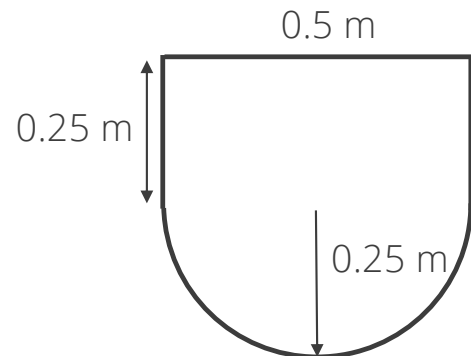
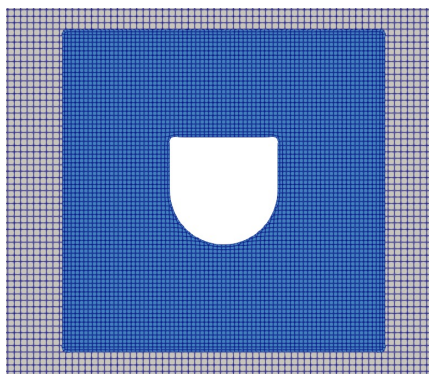


Hex8, Tet4, and Hex8/Tet4 Balanced Force
static bubble; density ratio = 1000



Validation: Unmoored Buoy Drop (Quiescent Conditions)

- Comparisons are made to experimental data from the UK Centre for Marine Energy Research (UKCMER) of the WEC vertical displacement given in Ransley et al., Renew. Ener. (2017) who exercised a mesh deformation construct



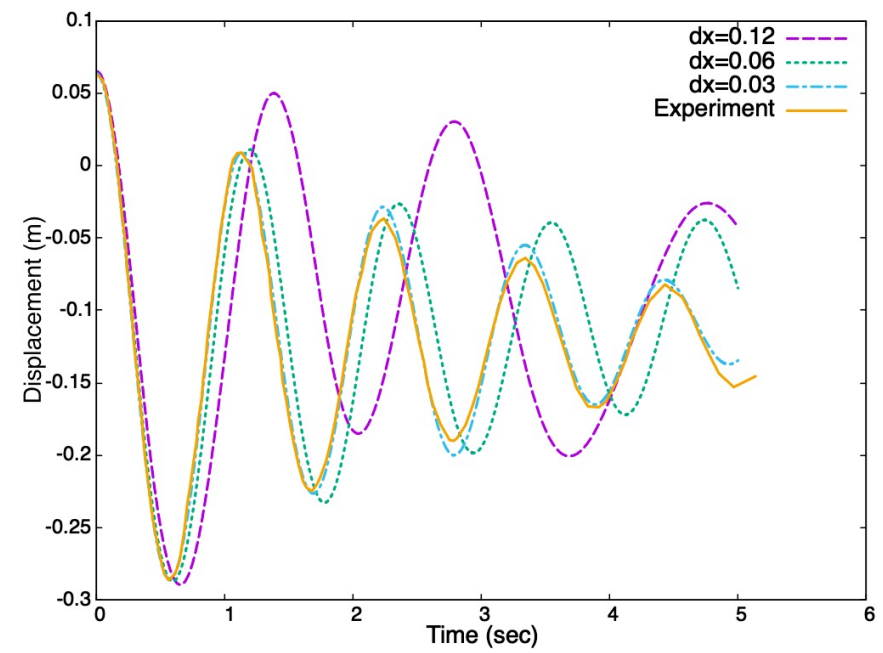
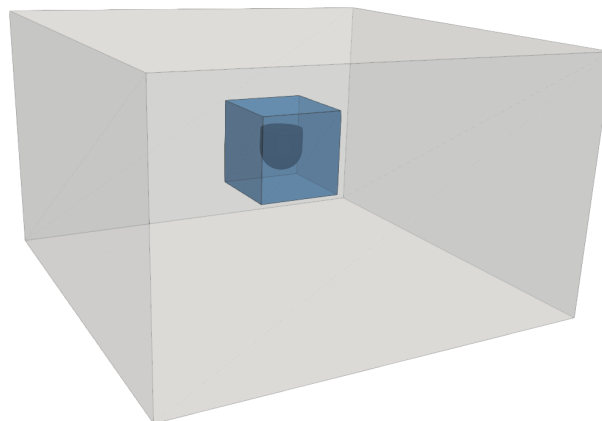
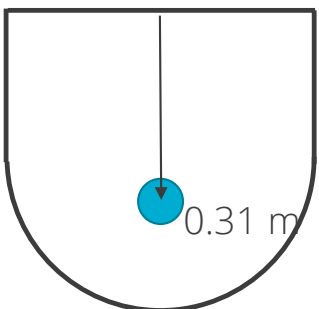


Validation: Unmoored Buoy Drop (Quiescent Conditions)

Objective: Compare to experimental dataset and demonstrate grid convergence

- Displaced buoy vertically; QoI: center of mass spatial location as a function of time

Finding: Improved comparison over other works found in literature, e.g., WEC vertical displacement given in Ransley et al., Renew. Ener. (2017)

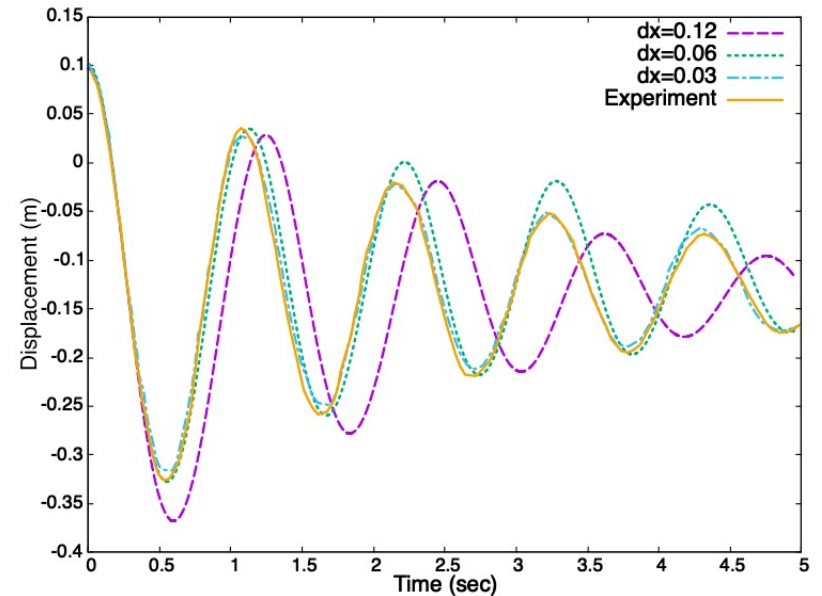
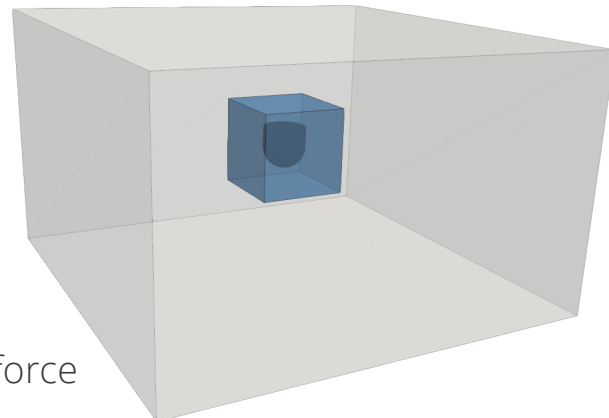
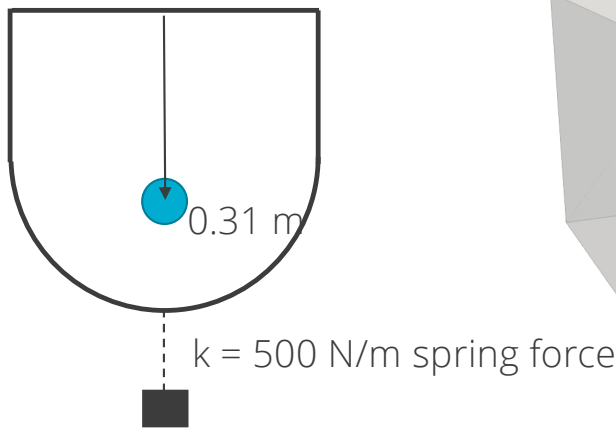


Validation: Moored Buoy Drop (Quiescent Conditions)

Objective: Compare to experimental dataset and demonstrate grid convergence – now tethered

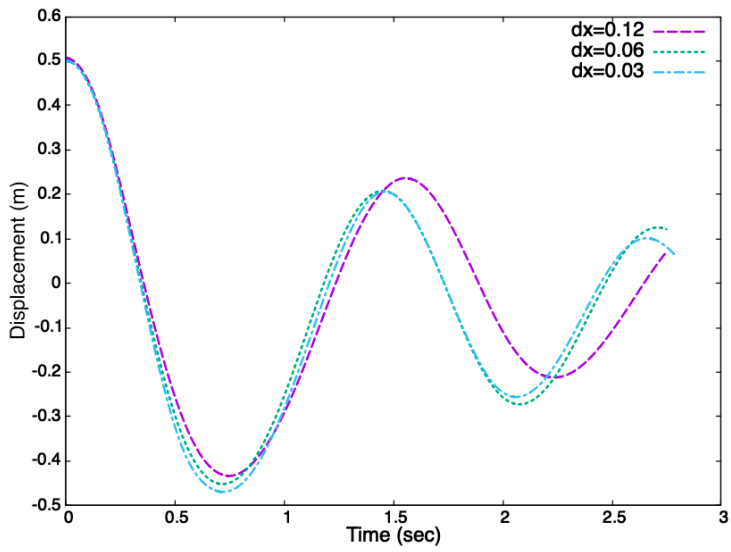
- Displaced buoy vertically; QoI: center of mass spatial location as a function of time

Similar Finding: Improved comparison over other works found in literature, e.g., WEC vertical displacement given in Ransley et al., Renew. Ener. (2017)

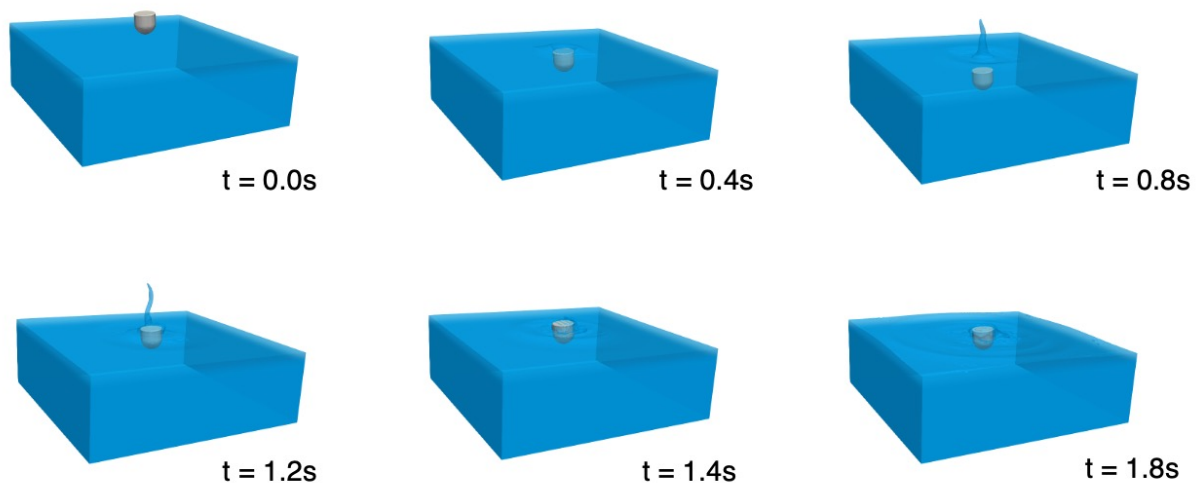




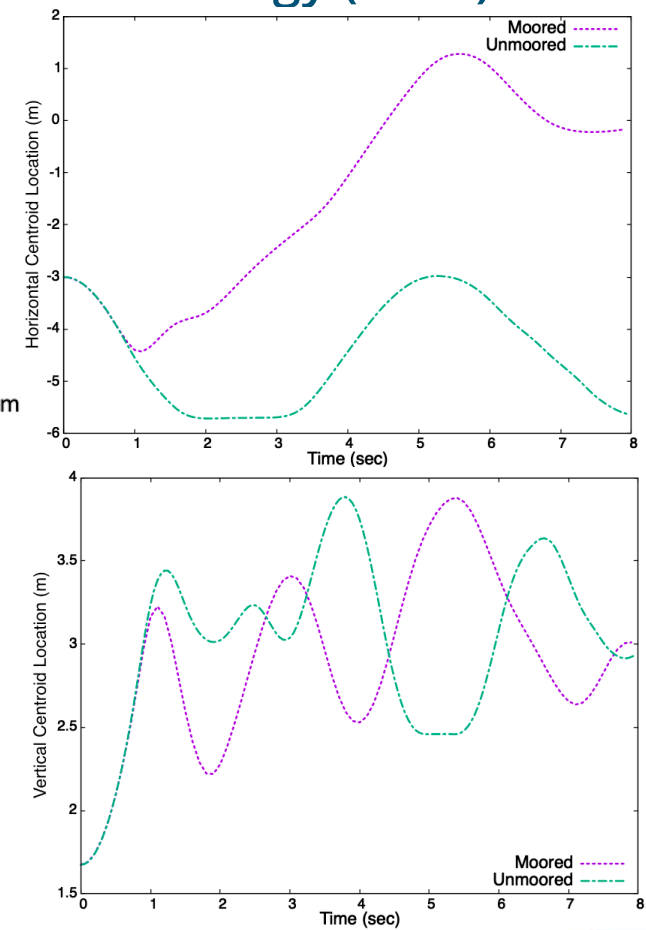
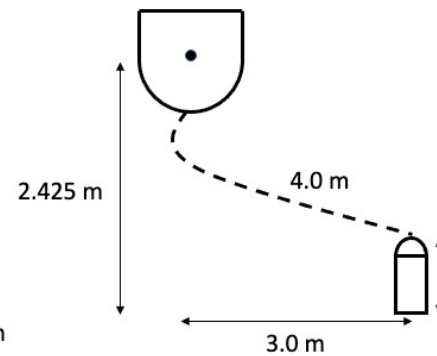
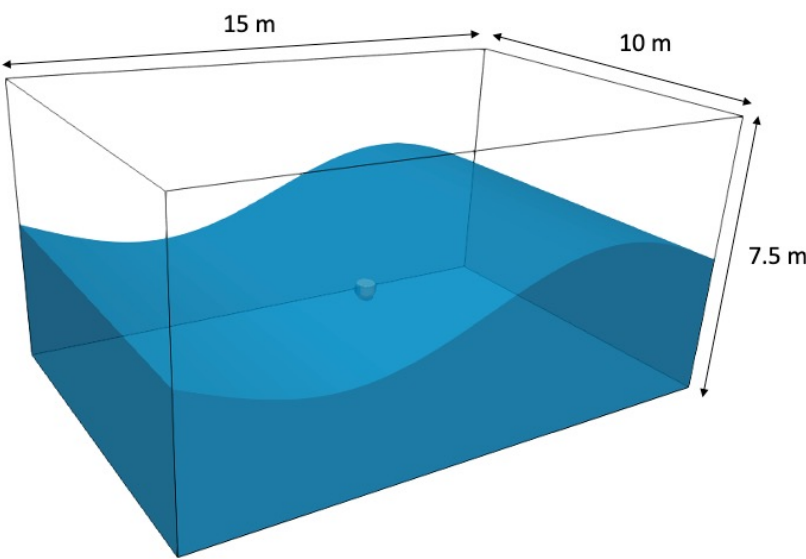
Buoy Dropped Into Quiescent Pool; large displacement limit Validation Benchmark, Domino and Horne, Renew. Energy (2022)



Large-displacement sample case run that can serve as a numerical benchmark



Buoy Subjected to large Wave-Form Validation Benchmark, Domino and Horne, Renew. Energy (2022)



- Large-displacement sample case run that can serve as a numerical benchmark for the community; with and without mooring
- Geometric center = $f(t)$ relative to the tether's mounting point



Buoy Subjected to large Wave-Form Validation Benchmark: Without (left) and With (right) Mooring

